Direct and sensitive miRNA profiling from low-input total RNA

Hui Wang, Robert A. Ach, and Bo Curry

RNA 2007 13: 151-159; originally published online Nov 14, 2006;
Access the most recent version at doi:10.1261/rna.234507

Direct and sensitive miRNA profiling from low-input total RNA

HUI WANG, ROBERT A. ACH, and BO CURRY
Agilent Technologies, Inc., Agilent Laboratories, Santa Clara, California 95051, USA

ABSTRACT

We have developed a sensitive, accurate, and multiplexed microRNA (miRNA) profiling assay that is based on a highly efficient labeling method and novel microarray probe design. The probes provide both sequence and size discrimination, yielding in most cases highly specific detection of closely related mature miRNAs. Using a simple, single-vial experimental protocol, 120 ng of total RNA is directly labeled using Cy3 or Cy5, without fractionation or amplification, to produce precise and accurate measurements that span a linear dynamic range from 0.2 amol to 2 fmol of input miRNA. The results can provide quantitative estimates of the miRNA content for the tissues studied. The assay is also suitable for use with formalin-fixed paraffin-embedded clinical samples. Our method allows rapid design and validation of probes for simultaneous quantitative measurements of all human miRNA sequences in the public databases and to new miRNA sequences as they are reported.

Keywords: miRNA profiling; microarray; RNA labeling; probe design; microRNA

INTRODUCTION

MicroRNAs (miRNAs) are a class of small single-stranded noncoding RNAs [19–30 nucleotides (nt)] that have been found in animals, plants, and viruses, with over 400 identified in humans (Bartel 2004; Griffiths-Jones 2004; Zamore and Haley 2005; Griffiths-Jones et al. 2006; Kim and Nam 2006). MicroRNA genes are transcribed as pri-miRNAs, which are then processed to the shorter hairpin shaped pre-miRNAs (~70–90 nt) before they are cleaved to form the mature single-stranded miRNAs (~22 nt) (Bartel 2004; Zamore and Haley 2005; Kim and Nam 2006). As part of a multiprotein RNA-induced silencing complex, the miRNAs repress translation by forming imperfect base pairing with the 3′ untranslated region of target messenger RNAs (mRNAs). Bioinformatics and cloning studies have estimated that miRNAs may regulate 30% of all human genes (Lewis et al. 2005; Lim et al. 2005). Recent studies have shown that distinct miRNA expression patterns are associated with various tumor types (Calin et al. 2004; Lu et al. 2005; Cummins et al. 2006; Esquela-Kerscher and Slack 2006).

The ardent interest in profiling miRNA expression has led to developments in Northern blot (Cummins et al. 2006), cloning (Lau et al. 2001), PCR (Chen et al. 2005), bead-based (Lu et al. 2005), SAGE-based (Cummins et al. 2006), and microarray-based methods (Babak et al. 2004; Barad et al. 2004; Calin et al. 2004; Liu et al. 2004; Nelson et al. 2004; Baskerville and Bartel 2005; Liang et al. 2005; Lim et al. 2005; Shingara et al. 2005; Castoldi et al. 2006). The ideal method would require submicrogram quantities of total RNA, have minimal sequence bias, be easy to multiplex, and involve simple experimental protocols. Microarray-based assays offer an efficient method for measuring the expression profile of large numbers of miRNAs simultaneously. However, the small size and high sequence homology of miRNAs present major challenges to sample labeling and microarray probe design.

Here we present a novel miRNA assay employing simple high-efficiency direct labeling of submicrogram quantities of total RNA, without amplification or size fractionation. Our labeling protocol has little sequence bias, and our in situ synthesized DNA microarray probes (Hughes et al. 2001) are both sequence and size selective for mature miRNAs. The enzymatic labeling attaches a single fluorophore-labeled nucleotide to the 3′ end of each miRNA with high yield and minimal sample manipulation. Hybridization to the microarray is carried out under conditions that result in near-equilibrium binding and high (>25%) hybridization yields for most miRNAs. The assay is easy to perform, has

Reprint requests to: Hui Wang, Agilent Technologies, Inc., Agilent Laboratories, 5301 Stevens Creek Boulevard, Santa Clara, CA 95051. USA; e-mail: hui_wang@agilent.com; fax: (408) 553-2161.

Article published online ahead of print. Article and publication date are at http://www.rnajournal.org/cgi/doi/10.1261/rna.234507.

low detection limits (<0.05 amol), and spans a $>10^4$ linear dynamic range (0.2 amol–2 fmol). The method described here also has the potential to provide quantitative measurements of miRNA copy numbers.

RESULTS

RNA labeling

Quantitative direct labeling methods that minimize sample manipulations, such as size separation or amplification, are most likely to produce accurate measurement of miRNA profiles. The small mature miRNA is an ideal substrate for T4 RNA ligase, though this enzyme can be sensitive to RNA sequence and secondary structures (England and Uhlenbeck 1978; Romaniuk et al. 1982; Romaniuk and Uhlenbeck 1983). To minimize the effect of structure and sequence differences among miRNAs, dimethylsulfoxide (DMSO), which is an effective RNA denaturant (Strauss et al. 1968), is added to the reaction solution. Up to 20% DMSO has been reported to stimulate T4 RNA ligase activity (Bruce and Uhlenbeck 1978; Romaniuk and Uhlenbeck 1983). By attaching a single cyanine dye to the 3′ phosphate of 3′, 5′-cytidine bisphosphate (pCp-Cy5 or pCp-Cy3), successful ligation produces an miRNA with an additional 3′cytidine and exactly one cyanine dye on its 3′end.

In order to determine the optimal DMSO concentration, DMSO was titrated into the ligation reaction. Several synthetic RNA oligonucleotides were labeled in the presence of 0%, 15%, and 25% DMSO, with and without pre-denaturation by heating and flash-cooling the RNA (see Supplement 1 for RNA sequence and yield data). Significant improvement in ligation yields was observed for 0% and 15% DMSO with pre-denaturation by heating. At 25% DMSO, similar yields were obtained with or without pre-denaturation, indicating a disruption of RNA secondary structure (Fig. 1A). With 25% DMSO, 53 individually labeled synthetic miRNAs showed no bias for pCp-Cy5 or pCp-Cy3 (Fig. 1B), though a slight 3′nucleotide bias was observed (Fig. 1C). The presence of a 10-fold excess of mixed competitor miRNAs did not affect labeling efficiency, and synthetic hairpin pre-miRNAs were not effectively labeled (data not shown).

Although synthetic miRNAs labeled with >80% yields, it is possible that these yields cannot be sustained in the presence of the complex RNA species present in biological samples. To address this possibility, 120–240 ng of total RNA from various human tissues were dephosphorylated and directly labeled with varying quantities of T4 RNA ligase (4–60 units) and pCp-dye (1–300 μM). Labeling efficiency was monitored by the microarray signals from pre- and post-label spiked-in synthetic miRNAs (0.2 amol–2 fmol) and by the consistency of measured tissue miRNA profiles. Reproducible spike-in signals and miRNA profiles were observed when the pCp-dye exceeded 1.4 nmol (50 μM) and the T4 RNA ligase exceeded 10 units (data not shown).

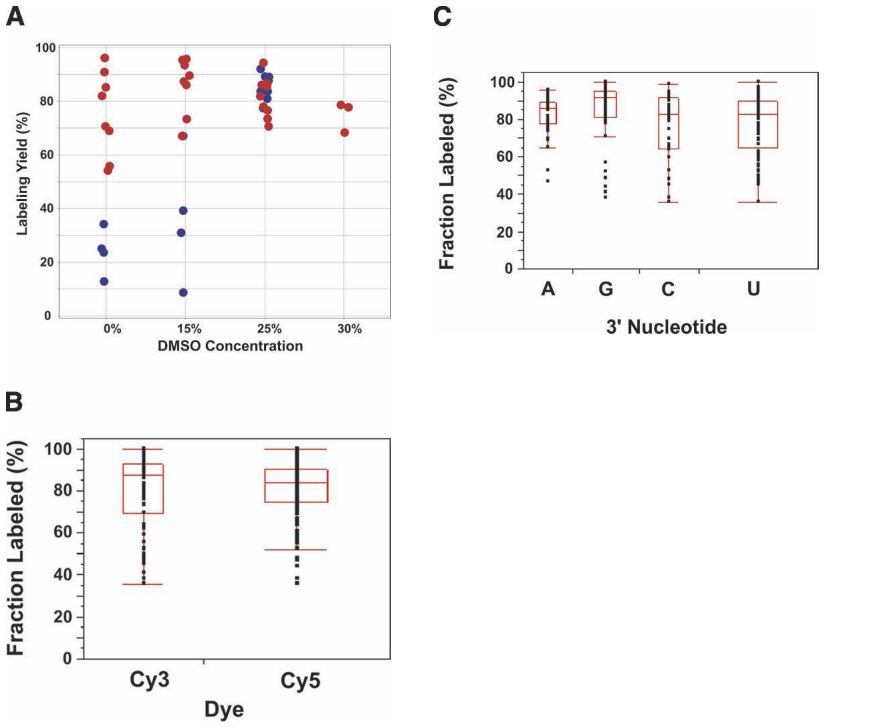

FIGURE 1. Validation of labeling efficiency. (*A*) Effect of DMSO. Five synthetic miRNAs containing different sequences were either directly labeled (blue) at 0%, 15%, or 25% DMSO or heated prior to labeling (red) at 0%, 15%, 25%, or 30% DMSO. At 25% DMSO, high labeling yields were observed independent of heat denaturation. Fifty-five separate reactions are shown. (*B*) Evaluation of dye bias. Box plots of labeling efficiencies of 53 different synthetic miRNAs labeled individually with Cy5-pCp and Cy3-pCp are shown. Results from 220 miRNA ligations are shown (see Supplement 1 for all detailed ligation data). The mean yield and standard error was 80±2 for Cy3 and 81±1 for Cy5. ANOVA *p* value of the Cy3 and Cy5 labeling efficiency distributions was 0.70, showing no difference between the labeling efficiencies of the two dyes. (*C*) Evaluation of sequence bias. Box plots of ligation efficiencies of the 220 reactions from *B* categorized according to 3′ nucleotide are shown. The mean percent yields of the labeled product and the standard errors were 82 ± 3 for A, 86 ± 2 for C, 78 ± 2 for G, and 78 ± 2 for U. ANOVA *p* value distinguishing the four distributions was 0.015, indicating that the labeling bias, while slight, is statistically significant. Ligations in *A* and *B* with low yields (<60%) were not reproducible, as subsequent ligations generally resulted in significantly higher yields (>80%). The reasons for these occasional instances of low yields are unclear. Infrequency and lack of reproducibility suggest such low yields are atypical experimental variations. High yields (>90%) were very reproducible.

Hybridized signals generally increased with increasing pCp-dye concentration, but no significant increase was observed beyond 2.8 nmol (100 μM). Stable miRNA expression profiles were obtained even with incomplete labeling (see Supplement 2 for details), consistent with independent, noncompetitive labeling of the different sequences in the complex RNA mixture.

Probe design and specificity

In a microarray hybridization, conditions are equally stringent for all targets measured. Therefore, when designing probes, it is important to equalize the melting temperatures (T_m) of the various probe–target hybrids. The small size of miRNAs requires a different strategy than that used for genomic or mRNA targets, where sequences with equal melting temperatures can be selected. Other workers have addressed the issue of T_m-balancing miRNA probes by incorporating modified nucleotides into probe sequences (Castoldi et al. 2006).

We were able to design efficient miRNA probes using only unmodified DNA oligonucleotides by utilizing several novel design features (Fig. 2A). First, a G is added to the 5′ end of each probe sequence to complement the 3′ cytosine introduced in labeling. This added G-C pair stabilizes the targeted miRNA relative to homologous RNAs. With the additional G-C interaction, nearly all mature miRNAs have calculated melting temperatures above 55°C under our hybridization conditions. Those miRNAs whose melting temperatures exceed 57.5°C are destabilized by reducing the hybridization length of the probes, starting from the 5′ end of the miRNA sequence. Since most of the sequence homology among miRNAs tends to be near the 5′ end (Griffiths-Jones 2004; Griffiths-Jones et al. 2006), sequentially eliminating base pairing from the 5′ end has little effect on probe sequence specificity.

To help distinguish the targeted miRNA from unintended potential targets, a hairpin structure is incorporated onto the 5′ end of the probe, directly abutting the 3′ end of the hybridizing sequence. The hairpin destabilizes hybridization to larger nontarget RNAs, and can provide additional stabilization if the target–probe duplex stacks with the probe hairpin.

The final step in our probe design strategy is empirical selection of the optimal probe length. For each miRNA sequence, all probe sequences with a calculated T_m (SantaLucia et al. 1996) between 50°C and 60°C were synthesized on microarrays both with and without the 5′ hairpin. The microarrays were then hybridized with synthetic and tissue RNAs at 50°C, 52.5°C, 55°C, 57.5°C, 60°C, and 65°C. The two sequences observed to melt just below and just above 57.5°C were included in subsequent array designs (see Supplement 3 for details and Supplement 4 for data). The data presented here were obtained from an experimental microarray containing 2–12 probes for each of the 314 human miRNAs listed in version 7.0 of the Sanger miRNA database (http://microrna.sanger.ac.uk; Griffiths-Jones 2004; Griffiths-Jones et al. 2006).

To examine the sequence specificity of our probes, 19 synthetic human miRNAs with high sequence homology to other miRNAs were individually labeled and hybridized. Very low (<1%) cross-hybridization was observed for miRNAs differing by >1 nt. Most miRNAs hybridized only to their specific probes (data not shown), although let-7a, -7b, -7c, -7e, miR-19b, -20b, and -30a-3p show >40% cross-hybridization. Typical specificity is illustrated by the let-7 family (Fig. 2B). Higher cross-hybridization was generally observed for single nucleotide purine-to-purine or pyrimidine-to-pyrimidine substitutions. Cross-hybridization between homologous sequences was asymmetric, as observed for let-7b and -7c. The data presented for these specificity studies study were not from an empirically T_m-matched array (for probe sequences, see Supplement 4). Fine tuning of probe T_m is expected to improve specificity, although it is unlikely to completely eliminate cross-hybridization in such multiplex hybridization measurements.

To reduce the complexity of biological samples, many investigators separate low-molecular-weight miRNAs from the more abundant higher-molecular-weight species before miRNA profiling (Barad et al. 2004; Thomson et al. 2004; Baskerville and Bartel 2005; Liang et al. 2005; Lu et al. 2005; Shingara et al. 2005). To test whether our labeling and hybridization are sufficiently selective to prevent pri-miRNAs, pre-miRNAs, and non-miRNAs from cross-hybridizing, miRNA expression profiles obtained from unfractionated total RNA were compared to those from total RNA that had been size fractionated by either conventional denaturing polyacrylamide gel electrophoresis (data not shown) or Flash-PAGE (Ambion; Fig. 2C). For all but a few miRNAs the correlation between signals from total and purified small RNAs was excellent, demonstrating that fractionation of the samples is not required. Total RNAs labeled with poly-A directed primers (Boorman et al. 2005) and larger RNAs (>40 nt) isolated from denaturing polyacrylamide gels and labeled with the T4 RNA ligase method described here yielded only a small number of sporadic signals on the miRNA microarrays and showed no correlation with miRNA signals from total or purified small RNA samples (data not shown). Hybridization of synthetic miRNAs was not affected by the presence of equal molar quantities of synthetic pre-miRNAs (data not shown).

Hairpin and nonhairpin probes exhibited similar empirical T_m for all miRNAs in the synthetic mixtures and for most miRNAs in the tissue samples. To understand the exceptions, we further investigated miR-494, which reported consistently stronger signals from the nonhairpin probes in the tissues examined (thymus, placenta, liver, heart, skeletal muscle). Northern blots of these total RNAs using a probe for miR-494 did not detect any RNAs the size of mature miR-494, but did detect several larger RNAs

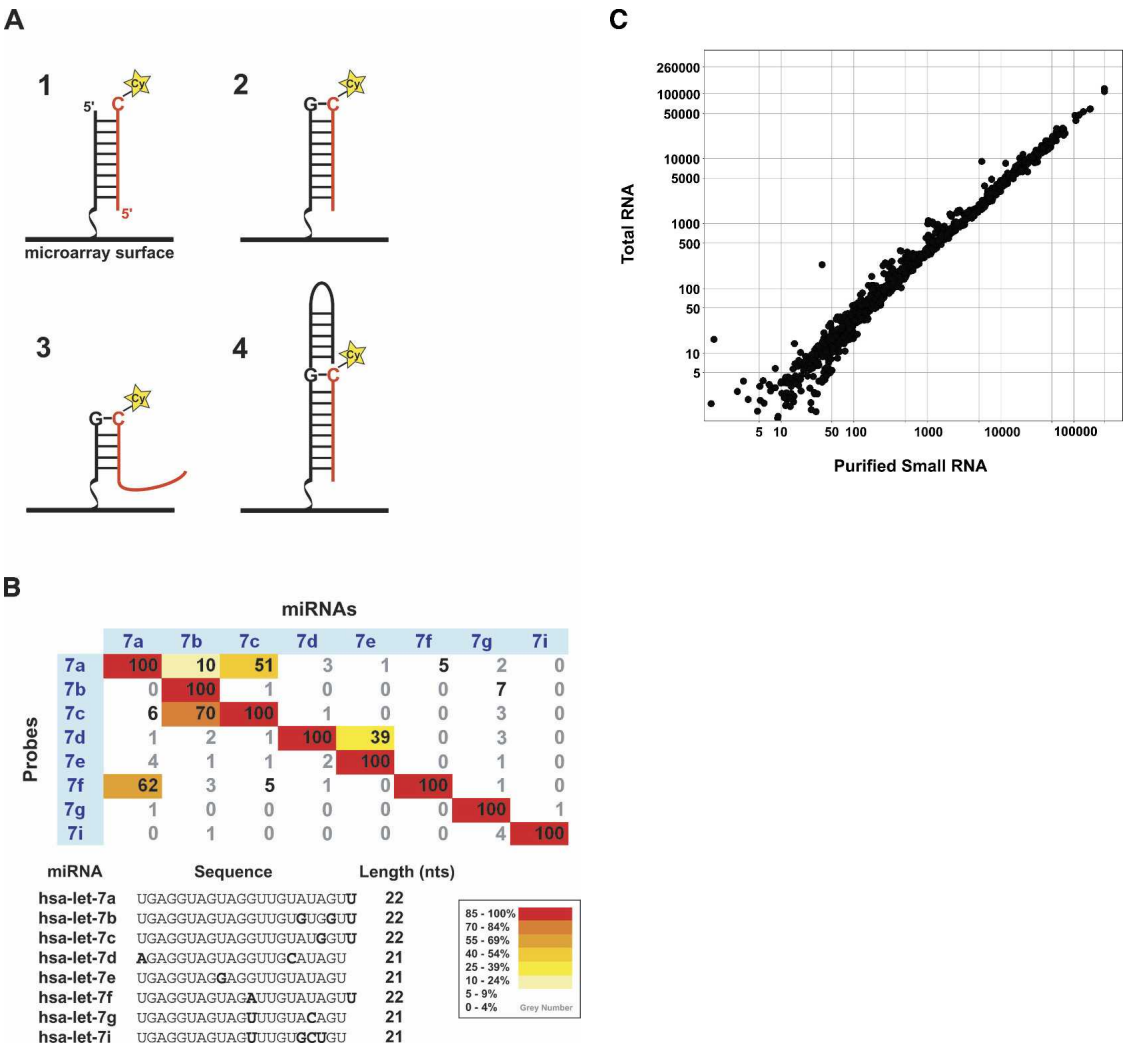

FIGURE 2. Probe design and specificity. (*A*) Schematic of the miRNA microarray probe design. Unmodified microarray probe (black) hybridized to miRNA target (red) is shown in (*1*), where the hybridizing sequence synthesized on the microarray (the probe) is connected to the glass surface by a T_{10} stilt (squiggly line). By adding a G on the 5′ end of the probe, one more G-C pair is added to the probe–target interaction (*2*). When necessary, destabilization of the probe–target hybrid is achieved by eliminating base-pairing from the 5′ end of the miRNA, by shortening the probe from the 3′ end (*3*). All probes were synthesized with and without hairpins (*4*), which can increase the specificity toward the target miRNA and can potentially increase the stability of probe–target interactions. (*B*) Probe–target sequence specificity of the human let-7 family. Each miRNA in the let-7 family was individually labeled and hybridized. The total signals reported by all the probes were normalized to the perfect match probe–target hybrid for each microarray. (*C*) Hybridization of FlashPAGE-enriched small RNA versus total RNA from placenta. Background-subtracted microarray signals from 60 ng of FlashPAGE-separated small RNAs (from 570 ng of total RNA) (*x*-axis) are plotted versus signals from 120 ng of total RNA (*y*-axis). Pearson correlation of the two samples is 0.992. The FlashPAGE separated and the total RNA were from the same placenta tissue and were labeled using the methods described here. Data are from both hairpin and nonhairpin probes.

(~0.5–2 kb; data not shown). Synthetic miR-494 hybridized in the absence of tissue samples reported equal signals from hairpin and nonhairpin probes, suggesting that the signal discrepancy between the hairpin and nonhairpin probes in the tissue RNA samples was due to the hybridization of larger RNAs to the nonhairpin probes. The tight correlations between size-fractionated and total RNA samples (Fig. 2C) indicate that, for the large majority of miRNAs, probe–target interactions are highly specific and independent of the hairpin structure. The hairpin architecture serves as an additional discriminating factor in the rare cases when longer RNAs are capable of hybridizing to the probes.

Sensitivity and dynamic range

Since miRNA expression levels have been reported to span over four orders of magnitude (Cummins et al. 2006), accurate miRNA profiling requires a system with a large linear dynamic range and high sensitivity. To determine the linear dynamic range of our assay, an equimolar mixture of 57 synthetic miRNAs was labeled and hybridized in

aliquots of 0.2 amol to 2 fmol of each miRNA (Fig. 3). The 57 synthetic sequences were selected based on predicted propensities for secondary structures, unusual or representative sequence composition, and exceptional calculated T_m. The slopes of the log–log plots of concentration versus signal were 1.04 ± 0.01, consistent with a linear response (see Supplement 5 for a detailed explanation). In nearly all cases the signals were proportional to the input miRNA concentrations over the entire range examined. Thus the detection limit of the assay is lower than 0.2 amol, and the linear dynamic range exceeds four orders of magnitude. Reported scanner counts/pixel can be converted to an absolute yield (fmol-detected/fmol-input), so that overall yields and detection limits for the 57 miRNAs can be directly calculated (see Supplement 6 for calculated yields).

While most of the miRNAs exhibited similar behavior, we observed a moderately large range of hybridization yields and a few distinct outliers, namely, miR-126*, miR-384, and miR-296. Both miR-126* and miR-384, whose calculated T_m were exceptionally low, reported low signals. The only sequence that failed to produce a linear response, miR-296, was selected for this study because its sequence contains seven consecutive internal cytosines. The G track in its probe was anticipated to aggregate and inhibit target hybridization. At quantities $>10^{-1}$ fmol, miR-296 is able to hybridize effectively. Other sequences that were predicted to have low hybridization yields because of exceptionally low T_m or possible secondary structures behaved as expected. Overall yields of more typical sequences, determined by calculating femtomole detected as a percentage of femtomole input, ranged from 15% to 40% with an average of 30%. Yields in this range are consistent with our probe design strategy. Higher hybridization yields could be achieved by choosing probes with higher T_m, but at the cost of reduced sequence specificity (see Supplement 5 for details).

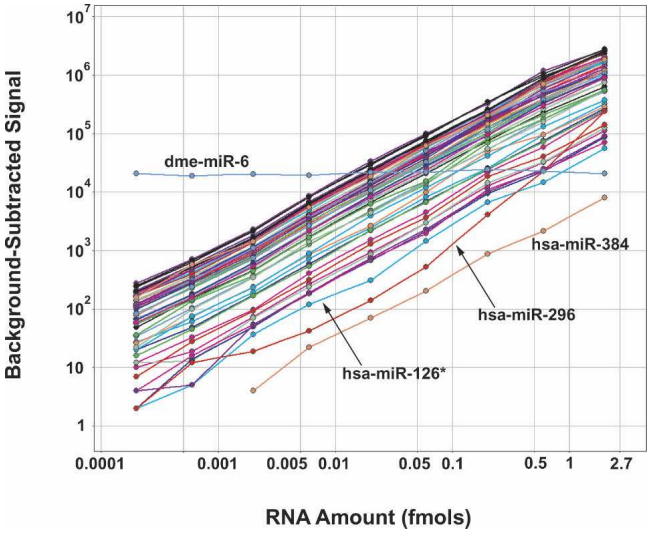

FIGURE 3. Linear dynamic range of microarray signals. An equimolar mixture of 57 synthetic miRNAs was labeled and hybridized in 0.2 amol to 2 fmol aliquots on individual microarrays. Prelabeled 0.2 fmol of dme-miR-6 was added as a control. All miRNAs behaved similarly, except for the three indicated. Both miR-126* and miR-384 had exceptionally low calculated T_m. The unusual sequence content of miR-296 inhibits hybridization at low concentrations, resulting in a nonlinear response. The slopes of the linear portions of the curves for all miRNAs are 1.04 ± 0.01 (1 SD). Data are background subtracted signals, not normalized, summed over all probes to each miRNA. The list of miRNAs and the data used to generate the figure are included in Supplement 6.

To confirm that the linear response observed in oligonucleotide mixtures is not compromised in complex mixtures, 0.2 amol to 2 fmol of synthetic *Drosophila* miRNAs, previously verified to cross-hybridize minimally with human miRNAs, were spiked into human total RNA before labeling. Prelabeled *Drosophila* miRNAs were also added to the complex sample after labeling. The signals observed for the spiked-in miRNAs correlated with those observed in the absence of tissue RNA (see Supplement 7 for data).

The minimal deviations from linearity observed in the titration curves of Figure 3 give an indication of the reproducibility of hybridization and wash on multiple arrays, as labeling variation is obviated. Signals measured for aliquots from pooled labeling reactions, measured on different arrays, generally agree within 10% (see Supplement 6).

MicroRNA profiles of tissues and preserved samples

The robustness and reproducibility of the signals is not limited to synthetic miRNAs. We measured miRNAs from total RNAs extracted from liver, heart, placenta, thymus, brain, skeletal muscle, and breast tissues. One hundred twenty to 240 ng of total RNA were labeled and hybridized onto one or two microarrays (60–240 ng total RNA per microarray). Measured miRNA expression profiles did not depend on the dye (Fig. 4A). Background-subtracted miRNA signals from a few to over 500,000 counts/pixel were observed in these samples, confirming the wide dynamic range of miRNA expression. Different tissues exhibit strong differential expression (Fig. 4B,C), and miRNA composition and quantity varies significantly among different tissues (Fig. 4C; see Supplement 8 for data).

Based on our studies with synthetic miRNAs (Fig. 3), the total mass of labeled miRNA hybridized can be estimated from the observed signals and the scanner calibration. For the samples measured, the hybridized miRNAs comprise 0.011% (brain), 0.012% (breast), 0.009% (heart), 0.003% (liver), 0.007% (thymus), and 0.025% (placenta) of the total RNA input by mass. Since only the 314 targeted miRNAs are included in this estimation and the mean labeling and hybridization yield measured for the synthetic miRNA cocktail is about 30%, these quantities likely underestimate the total miRNA fraction by 3× or more.

For comparison, we measured the relative amounts of 10 different miRNAs in seven different human tissues using

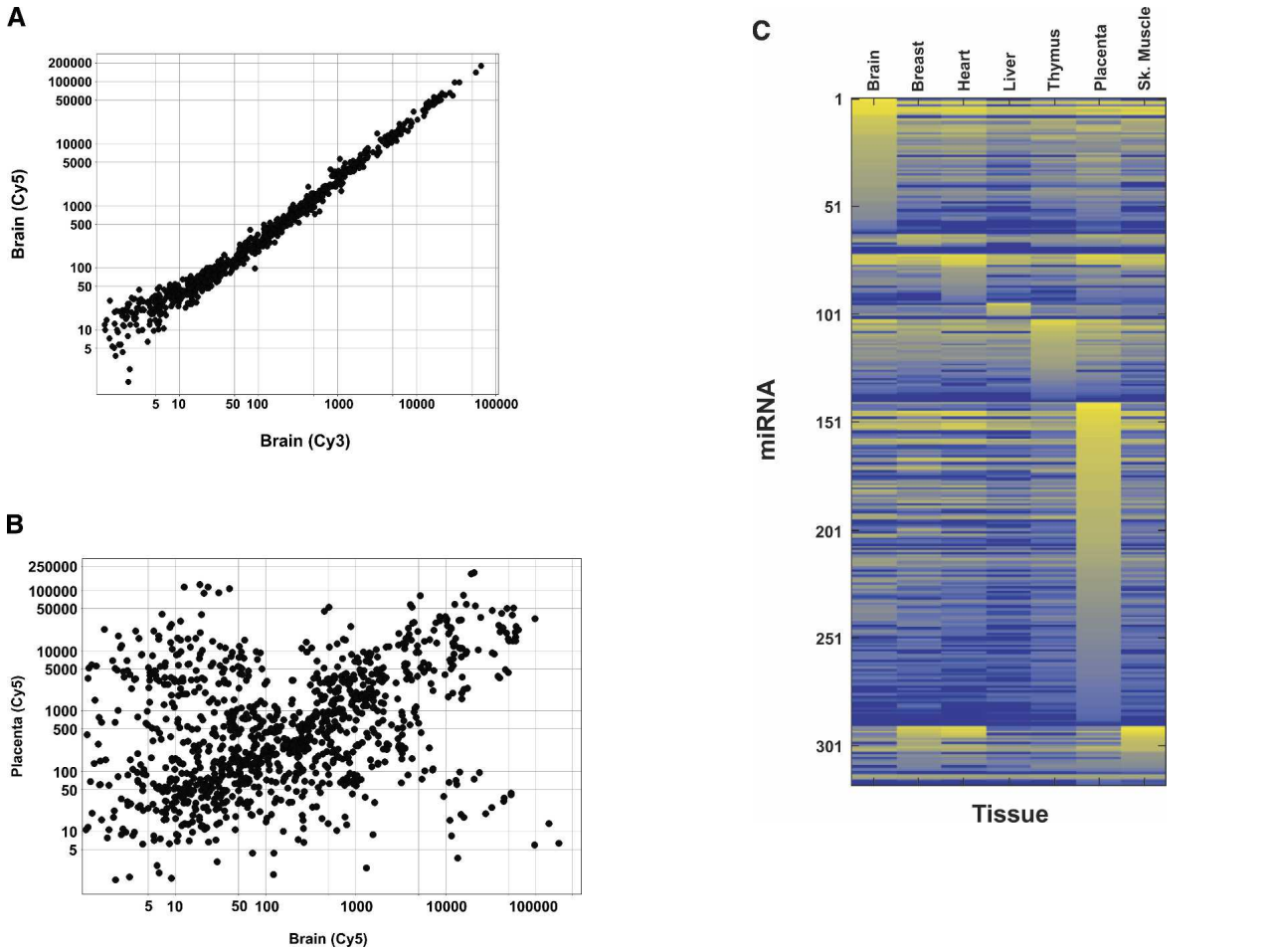

FIGURE 4. miRNA expression profiles of human tissue total RNAs. All data were background-subtracted signals from hairpin and nonhairpin probes, obtained from 120 ng of total RNA. (*A*) miRNA expression profiles of human brain tissue from two separate labeling reactions. Pearson correlation for the data shown is 0.994. Highly reproducible miRNA profiles were obtained for all tissues examined. (*B*) Differential expression profile between placenta and brain. Pearson correlation between the samples is 0.238. (*C*) Heat map of miRNA expression profiles from human brain, breast, heart, liver, thymus, placenta, and skeletal muscle tissues. The color is proportional to the logarithm of measured signals, from blue (no detectable signal) to yellow (highest signal). Signals from *Drosophila* miRNA probes are on the *bottom* four rows of the map; the spiked-in *Drosophila* sequences appear as uniform yellow lines across the heat map while the sequences that were not spiked-in appear as uniform blue lines.

quantitative RT-PCR (Fig. 5). The microarray results clearly correlated with the qPCR results.

To check the applicability of our system to preserved tissue RNAs, which are a rich source of samples for clinical studies, we compared results from frozen and formalin-fixed paraffin-embedded (FFPE) samples taken from the same breast tumors. Pearson correlations for five pairs of frozen and FFPE samples were 0.443, 0.836, 0.816, 0.927, and 0.911. Frozen and FFPE RNA samples yielded similar signal levels (data not shown).

DISCUSSION

The labeling, probe design, and hybridization protocol described here is simple, sensitive, and largely immune to sample-dependent biases. Our assay can measure miRNA directly in complex samples with high yield and specificity because it minimizes sample manipulation, integrates direct labeling of RNA with probe design, and empirically matches probe–target T_m to hybridization conditions. The dephosphorylation and direct labeling of total RNA in the same sample tube is straightforward and requires very low RNA input compared to other methods in current use (Babak et al. 2004; Barad et al. 2004; Calin et al. 2004; Liu et al. 2004; Nelson et al. 2004; Thomson et al. 2004; Baskerville and Bartel 2005; Liang et al. 2005; Lim et al. 2005; Lu et al. 2005; Shingara et al. 2005; Castoldi et al. 2006). Our method is also applicable to labeling of unstructured single-stranded short RNAs other than miRNAs. Our probe design method allows us to rapidly design probes for new miRNA sequences as they are discovered.

An assay that directly utilizes total RNA minimizes the inevitable sample losses in more complex protocols requiring RNA size fractionation or multiple purification

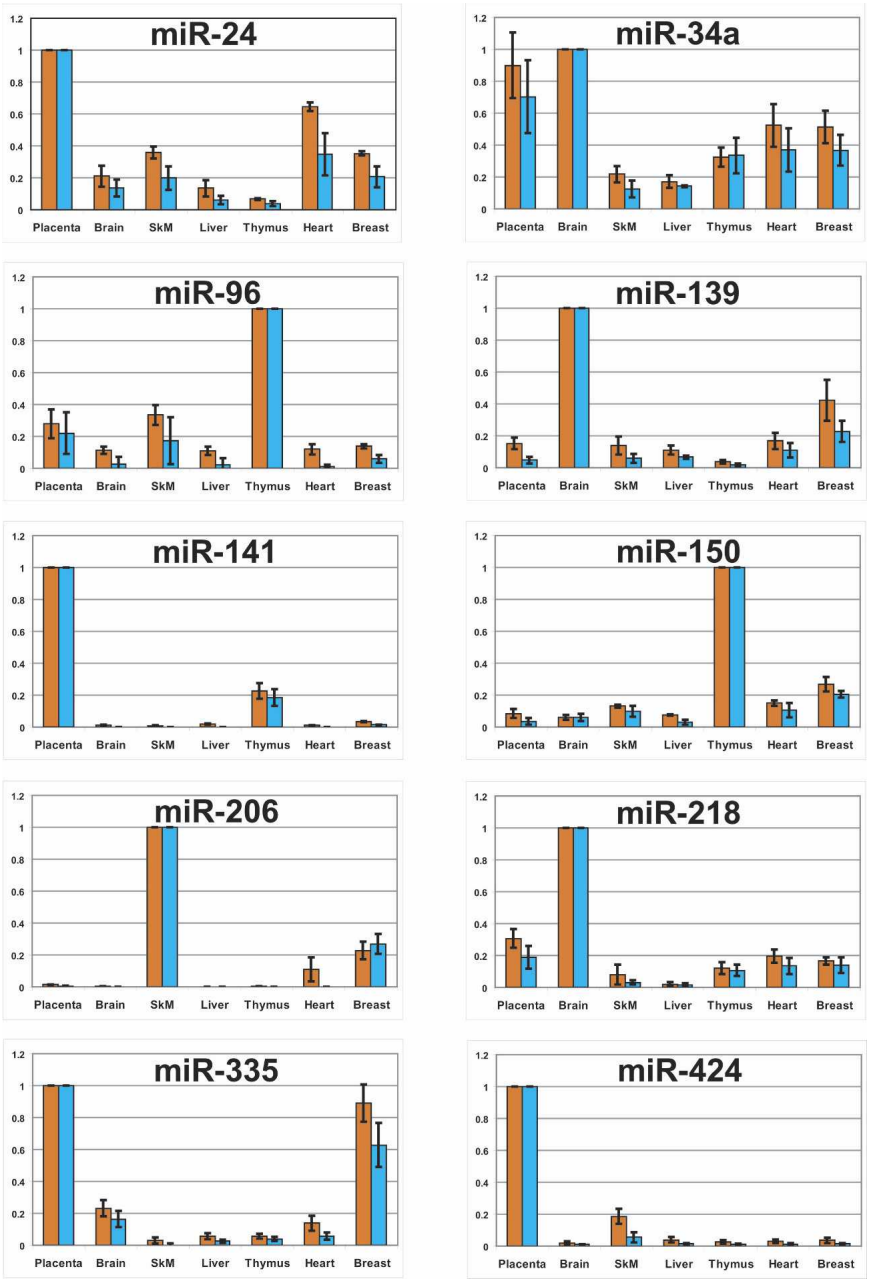

FIGURE 5. Comparison of quantitative RT-PCR (qRT-PCR) and microarray expression profiles of 10 miRNAs. Relative expression of 10 human miRNAs was determined for seven different human tissues using both qRT-PCR and our microarray assay. Results are individually plotted for each miRNA, with qRT-PCR results in orange and microarray results in blue. The miRNA levels in each tissue are reported as the fraction of the expression level in the tissue in which that miRNA is most abundant. The qRT-PCR and the microarray results agreed on which tissue expressed the highest levels of each miRNA. The qRT-PCR reactions and microarray hybridizations were each repeated four times for each miRNA. Error bars indicate one standard deviation.

steps. For example, the consistently lower signals observed from size-fractionated samples, relative to those from the same input amount of total RNA, suggest a consistent loss of miRNA during size fractionation (Fig. 2C).

One advantage of the end-labeling method presented here is that it should be relatively insensitive to nucleotide damage in the substrate RNA, unless the damage occurs at the 3′ end. This contrasts with polymerase-based labeling methods, which can be vulnerable to any nucleotide modification along the target sequence. For this reason, our labeling technique may be particularly advantageous when used to label preserved or chemically treated samples.

In humans, translation inhibition mediated by miRNAs mainly occurs in a combinatorial manner, where each miRNA is capable of binding to more than one mRNA and each mRNA must be bound by multiple miRNAs for effective translation repression (Zamore and Haley 2005). Because of the cooperative role played by miRNAs in regulation of mRNA translation, the relative amounts of different miRNAs in a cell can be of fundamental biological importance. Accurate copy number measurements would greatly facilitate research into the molecular mechanisms by which miRNAs influence cellular growth and differentiation. There is thus a need for a quantitative assay capable of measuring expression of all miRNAs simultaneously.

A quantitative assay requires that each step proceed in reproducibly high yield and be insensitive to small deviations from the standard protocol. These goals are facilitated if there are no amplification or separation steps that can introduce sample-dependent variations and if both labeling and hybridization reach stable endpoints near equilibrium, minimally dependent on reaction kinetics or concentrations. Our labeling reaction adds exactly one fluorophore to each miRNA in reproducibly high yield, under conditions that are insensitive to small variations in pCp-dye or miRNA concentration. Hybridization is allowed to proceed far toward equilibrium, and the probe T_m matching ensures that most miRNAs will be predominately hybridized at equilibrium. The scanner calibration allows an accurate measurement of the number of hybridized labeled targets. Thus the method presented

here can serve as the foundation for the future development of a truly quantitative, fully multiplexed miRNA assay.

MATERIALS AND METHODS

RNA sources

Synthetic miRNAs were obtained from Dharmacon and Ambion. Total RNAs from human heart, skeletal muscle, breast, brain, thymus, liver, and placenta were from Ambion. Frozen and FFPE breast tumor total RNAs were from Michael Bittner (Translational Genomics Research Institute).

Size fractionation

Total RNA samples were size fractionated using the Ambion Flash-PAGE system according to the manufacturer's protocol or by using denaturing 20% polyacrylamide gels.

RNA labeling and hybridization

All enzymes were from Amersham, and reactions were performed with supplied buffer and BSA, unless otherwise specified. All enzymes are as described by the manufacturer. The pCp-Cy5 and pCp-Cy3 were made by conjugating Cy5 or Cy3 (Amersham) to the 3′ phosphate of pCp (Dharmacon). Labeling efficiency was optimized with 20 pmol synthetic miRNAs using T4 RNA ligase, 1 nmol pCp-Cy5 or pCp-Cy3 and 0%, 15%, 25%, or 30% (v/v) DMSO (Sigma) in 10 μL, which was then labeled with ^{32}P using T4 polynucleotide kinase, analyzed on a denaturing 20% polyacrylamide gel, and quantitated by PhosphorImager (Molecular Dynamics). For miRNA profiling, 120 ng of tissue total RNA, 60 ng of fractionated tissue RNA, or 120 ng of preserved tumor RNA were dephosphorylated with 16 units calf intestine alkaline phosphatase for 30 min at 37°C. The reaction was terminated at 100°C for 5 min and immediately cooled to 0°C. Seven microliters of DMSO were then added and heated to 100°C for 3 min and immediately cooled to 0°C. Ligase buffer and BSA were added and ligation was performed with 50 μM pCp-Cy5 or pCp-Cy3 and 15 units T4 RNA ligase in 28 μL at 16°C overnight. The labeled miRNAs were desalted with MicroBioSpin6 columns (BioRad) and combined with 4.5 μg of random DNA 25-mers (Operon). Some 22.5 μL 2× hybridization buffer (Agilent) was added to the labeled mixture to a final volume of 45 μL. The mixture was heated for 5 min at 100°C and immediately cooled to 0°C. Each 45 μL sample was hybridized onto a microarray at 55°C for 20–48 h. Time course experiments showed that hybridization is essentially complete after 40 h (data not shown). Slides were washed 10 min in 6× SSC/0.005% Triton X-102, then for 5 min in 0.1× SSC/0.005% Triton X-102, both at room temperature. Slides were scanned on an Agilent microarray scanner (model G2565A) at 100% and 5% sensitivity settings. Agilent Feature Extraction software version 8.1 was used for image analysis (see Supplement 9 for the detailed protocol).

Probe and microarray design

Custom microarrays were manufactured by Agilent Technologies (Hughes et al. 2001). Each slide contained eight individual microarrays, each with 1900 features. Arrays included 48 negative control features, used to estimate fluorescence background and background variance. Approximately 1400 features targeted 314 human miRNAs and five *Drosophila* miRNAs. Each miRNA was targeted by 2–12 array features containing probes of varying lengths, half of which contained the hairpin loops depicted in Figure 2A. The 3′ end of each probe was spaced away from the array surface with a T_{10} stilt (see Supplement 9 for the detailed protocol).

T_m determination

All probe lengths whose calculated DNA–DNA duplex T_m (SantaLucia et al. 1996) lay between 50°C and 60°C were synthesized on screening arrays. Probes for miRNAs whose full-length sequence had low calculated T_m (<50°C) were designed for both the full-length sequence (including the ligated 3′ C) and the sequence shortened by one base (from 5′ end). The actual T_m of the candidate probes were determined by hybridization of various tissue samples and synthetic miRNAs at temperatures between 50°C and 65°C (Supplement 4). The procedure used to deduce a melting temperature from these data is described in detail in Supplement 3. Probes observed to melt between 55°C and 57.5°C were included in subsequent array designs.

PCR validation

Quantitative RT-PCR validation was performed using SuperTaq polymerase and mirVana qRT-PCR miRNA detection kit and primers, following the manufacturer's protocol (Ambion). Standard curves were generated using 0.02–200 ng of total RNA from the tissue expressing the highest level of each particular miRNA. Reactions were performed on an ABI7700 thermocycler (Applied Biosystems), and cycle threshold values determined by the manufacturer's software.

SUPPLEMENTAL MATERIAL

All supplements are available at http://www.opengenomics.com/miRNA_Wang_etal_RNA2006_supplements.

ACKNOWLEDGMENTS

We thank Dr. Michael Bittner for the FFPE samples, Dr. Jeff Sampson for early support and for the probe hairpin sequence design, Dr. Nick Sampas for T_m calculation software, Dr. Brian Peter for critical reading of the manuscript, and Dr. Steve Laderman and Dr. Laurakay Bruhn for their consistent support and detailed discussions in the preparation of the manuscript.

Received July 19, 2006; accepted October 2, 2006.

REFERENCES

Babak, T., Zhang, W., Morris, Q., Blencowe, B.J., and Hughes, T.R. 2004. Probing microRNAs with microarrays: Tissue specificity and functional inference. *RNA* **10:** 1813–1819.

Barad, O., Meiri, E., Avniel, A., Aharonov, R., Barzilai, A., Bentwich, I., Einav, U., Gilad, S., Hurban, P., Karov, Y., et al. 2004. MicroRNA expression detected by oligonucleotide microarrays: System establishment and expression profiling in human tissues. *Genome Res.* **14:** 2486–2494.

Bartel, D.P. 2004. MicroRNAs: Genomics, biogenesis, mechanism, and function. *Cell* **116:** 281–297.

Baskerville, S. and Bartel, D.P. 2005. Microarray profiling of microRNAs reveals frequent coexpression with neighboring miRNAs and host genes. *RNA* **11:** 241–247.

Boorman, G.A., Irwin, R.D., Vallant, M.K., Gerken, D.K., Lobenhofer, E.K., Hejtmancik, M.R., Hurban, P., Brys, A.M., Travlos, G.S., Parker, J.S., et al. 2005. Variation in the hepatic gene expression in individual male Fischer rats. *Toxicol. Pathol.* **33:** 102–110.

Bruce, A.G. and Uhlenbeck, O.C. 1978. Reactions at the termini of tRNA with T4 RNA ligase. *Nucleic Acids Res.* **5:** 3665–3677.

Calin, G.A., Liu, C.G., Sevignani, C., Ferracin, M., Felli, N., Dumitru, C.D., Shimizu, M., Cimmino, A., Zupo, S., Dono, M., et al. 2004. MicroRNA profiling reveals distinct signatures in B cell chronic lymphocytic leukemias. *Proc. Natl. Acad. Sci.* **101:** 11755–11760.

Castoldi, M., Schmidt, S., Benes, V., Noerholm, M., Kulozik, A.E., Hentze, M.W., and Muckenthaler, M.U. 2006. A sensitive array for microRNA expression profiling (miChip) based on locked nucleic acids (LNA). *RNA* **12:** 913–920.

Chen, C., Ridzon, D.A., Broomer, A.J., Zhou, Z., Lee, D.H., Nguyen, J.T., Barbisin, M., Xu, N.L., Mahuvakar, V.R., Andersen, M.R., et al. 2005. Real-time quantification of microRNAs by stem-loop RT-PCR. *Nucleic Acids Res.* **33:** e179.

Cummins, J.M., He, Y., Leary, R.J., Pagliarini, R., Diaz Jr., L.A., Sjoblom, T., Barad, O., Bentwich, Z., Szafranska, A.E., Labourier, E., et al. 2006. The colorectal microRNAome. *Proc. Natl. Acad. Sci.* **103:** 3687–3692.

England, T.E. and Uhlenbeck, O.C. 1978. Enzymatic oligoribonucleotide synthesis with T4 RNA ligase. *Biochemistry* **17:** 2069–2076.

Esquela-Kerscher, A. and Slack, F.J. 2006. Oncomirs—MicroRNAs with a role in cancer. *Nat. Rev. Cancer* **6:** 259–269.

Griffiths-Jones, S. 2004. The microRNA Registry. *Nucleic Acids Res.* **32:** D109–D111.

Griffiths-Jones, S., Grocock, R.J., van Dongen, S., Bateman, A., and Enright, A.J. 2006. miRBase: MicroRNA sequences, targets and gene nomenclature. *Nucleic Acids Res.* **34:** D140–D144.

Hughes, T.R., Mao, M., Jones, A.R., Burchard, J., Marton, M.J., Shannon, K.W., Lefkowitz, S.M., Ziman, M., Schelter, J.M., Meyer, M.R., et al. 2001. Expression profiling using microarrays fabricated by an ink-jet oligonucleotide synthesizer. *Nat. Biotechnol.* **19:** 342–347.

Kim, V.N. and Nam, J.W. 2006. Genomics of microRNA. *Trends Genet.* **22:** 165–173.

Lau, N.C., Lim, L.P., Weinstein, E.G., and Bartel, D.P. 2001. An abundant class of tiny RNAs with probable regulatory roles in *Caenorhabditis elegans*. *Science* **294:** 858–862.

Lewis, B.P., Burge, C.B., and Bartel, D.P. 2005. Conserved seed pairing, often flanked by adenosines, indicates that thousands of human genes are microRNA targets. *Cell* **120:** 15–20.

Liang, R.Q., Li, W., Li, Y., Tan, C.Y., Li, J.X., Jin, Y.X., and Ruan, K.C. 2005. An oligonucleotide microarray for microRNA expression analysis based on labeling RNA with quantum dot and nanogold probe. *Nucleic Acids Res.* **33:** e17.

Lim, L.P., Lau, N.C., Garrett-Engele, P., Grimson, A., Schelter, J.M., Castle, J., Bartel, D.P., Linsley, P.S., and Johnson, J.M. 2005. Microarray analysis shows that some microRNAs downregulate large numbers of target mRNAs. *Nature* **433:** 769–773.

Liu, C.G., Calin, G.A., Meloon, B., Gamliel, N., Sevignani, C., Ferracin, M., Dumitru, C.D., Shimizu, M., Zupo, S., Dono, M., et al. 2004. An oligonucleotide microchip for genome-wide microRNA profiling in human and mouse tissues. *Proc. Natl. Acad. Sci.* **101:** 9740–9744.

Lu, J., Getz, G., Miska, E.A., Alvarez-Saavedra, E., Lamb, J., Peck, D., Sweet-Cordero, A., Ebert, B.L., Mak, R.H., Ferrando, A.A., et al. 2005. MicroRNA expression profiles classify human cancers. *Nature* **435:** 834–838.

Nelson, P.T., Baldwin, D.A., Scearce, L.M., Oberholtzer, J.C., Tobias, J.W., and Mourelatos, Z. 2004. Microarray-based, high-throughput gene expression profiling of microRNAs. *Nat. Methods* **1:** 155–161.

Romaniuk, P.J. and Uhlenbeck, O.C. 1983. Joining of RNA molecules with RNA ligase. *Methods Enzymol.* **100:** 52–59.

Romaniuk, E., McLaughlin, L.W., Neilson, T., and Romaniuk, P.J. 1982. The effect of acceptor oligoribonucleotide sequence on the T4 RNA ligase reaction. *Eur. J. Biochem.* **125:** 639–643.

SantaLucia Jr., J., Allawi, H.T., and Seneviratne, P.A. 1996. Improved nearest-neighbor parameters for predicting DNA duplex stability. *Biochemistry* **35:** 3555–3562.

Shingara, J., Keiger, K., Shelton, J., Laosinchai-Wolf, W., Powers, P., Conrad, R., Brown, D., and Labourier, E. 2005. An optimized isolation and labeling platform for accurate microRNA expression profiling. *RNA* **11:** 1461–1470.

Strauss Jr., J.H., Kelly, R.B., and Sinsheimer, R.L. 1968. Denaturation of RNA with dimethyl sulfoxide. *Biopolymers* **6:** 793–807.

Thomson, J.M., Parker, J., Perou, C.M., and Hammond, S.M. 2004. A custom microarray platform for analysis of microRNA gene expression. *Nat. Methods* **1:** 47–53.

Zamore, P.D. and Haley, B. 2005. Ribo-gnome: The big world of small RNAs. *Science* **309:** 1519–1524.